Size and shape of the repetitive domain of high molecular weight wheat gluten proteins. II. Hydrodynamic studies

van Swieten, E; Friesen, RR; de Kruif, CG; Robillard, GT; Kruif, Cees G. de

Published in:
Biopolymers

DOI:
10.1002/bip.10369

Publication date:
2003

Eric van Swieten[1,*]
Robert R. Friesen[1,†]
Cees G. de Kruif[2]
George T. Robillard[1,†]
[1] *University of Groningen, Department of Biochemistry, and Groningen Biomolecular Sciences and Biotechnology Institute, Nijenborgh 4, 9747 AG Groningen, The Netherlands*

[2] *Netherlands Institute of Dairy Research (NIZO) P. O. Box 20, 6710 BA, Ede, The Netherlands*

Received 9 January 2002; accepted 16 December 2002

Size and Shape of the Repetitive Domain of High Molecular Weight Wheat Gluten Proteins. II. Hydrodynamic Studies

Abstract: *This study describes the hydrodynamic properties of the repetitive domain of high molecular weight (HMW) wheat proteins, which complement the small-angle scattering (SANS) experiments performed in the first paper of this series. The sedimentation coefficients,* s_o*, and diffusion coefficients,* D_o*, were obtained from the homologuous HMW proteins dB1 and dB4 that were cloned from the gluten protein HMW Dx5, and expressed in* Escherichia coli*. Monodisperse conditions for accurate determination of* s_o *and* D_o*, were obtained by screening a series of buffers using dynamic light scattering. For the first time, hydrodynamic parameters were obtained on monodisperse samples that enabled the determination of the monomeric size and shape. The hydrodynamic values determined on dB1 and dB4 were used to test the worm-like chain (WLC) model that was proposed in the SANS studies. The successful matching of two separately obtained hydrodynamic parameters of dB1 and dB4 using the WLC model provides further evidence for the WLC model. The small discrepancy between the hydrodynamic and scattering data, possibly coming from the excluded volume effect, was compensated by a solvation layer of 1–2 water molecules thick around the protein in the WLC model. The solvation of the central domain is much higher than those of the terminal domains of the HMW subunits. This difference emphasizes the dual role of HMW*

Correspondence to: George T. Robillard; email: robillard@biomade.nl

Contract grant sponsor: Dutch Ministry of Economic Affairs
Contract grant number: IOP-IE92014

**Present address:* Heineken Technical Services, Research & Development, P. O. Box 510, 2380 BB, Zoeterwoude, The Netherlands

†*Present address:* BiOMaDe Technology Foundation, Nijenborgh 4, 9747 AG Groningen, The Netherlands

Biopolymers, Vol. 69, 325–332 (2003)

wheat gluten proteins in water-binding and aggregation. © 2003 Wiley Periodicals, Inc. Biopolymers 69: 325–332, 2003

Keywords: *high molecular weight; wheat gluten proteins; small-angle scattering; hydrodynamics; dynamic light scattering; worm-like chain*

INTRODUCTION

In the small-angle scattering (SANS) article, we have proposed a flexible worm-like chain (WLC) structure based on small-angle neutron and x-ray scattering experiments. The studies were performed on the homologuous proteins dB1 and dB4 that were cloned from the gluten protein high molecular weight (HMW) Dx5, and expressed in *Escherichia coli.* It was demonstrated that the monodisperse conditions were crucial for a proper determination of size and shape. The most suitable conditions for the SANS experiments were determined with dynamic light scattering, and are described in this article. In addition, we have determined two hydrodynamic parameters of both dB1 and dB4; the sedimentation coefficients, s_0, and diffusion coefficients, D_0, using analytical ultracentrifugation and dynamic light scattering (DLS), respectively. The results were compared with experimental s_0 and D_0 values of reference proteins, and frictional ratios were calculated. The hydrodynamic values determined on dB1 and dB4 were used to test the proposed WLC model, and other geometric models like the prolate ellipsoid and rod, that were frequently proposed in other studies as model for the repetitive domain of HMW gluten proteins.

RESULTS

Dynamic Light Scattering

Screening of Buffers. Although 2–10 mg/mL solutions of dB1 in 10–20 m*M* phosphate buffers looked perfectly clear by visual inspection, a rapid increase of scattering intensity was observed immediately after filtration of the sample. DLS showed the increase of count rate during 18 min for dB1 samples in phosphate buffers, directly recorded after filtration of the solution. A typical example is shown in Figure 1a.

Multiexponential fitting of nine consecutive runs of 2 min yielded mainly two population of particles of well-separated sizes. The contribution to the scattering signal effected by particles in the size range of dB1 decreased in time, whereas the signal of much larger particles increased to roughly 95% of the total intensity. The average Stokes radii (spheres) of the two populations were 31 and 1180 Å, respectively. Evidently, sonication or repeated filtration of dB1 in phosphate reduced the count rate only for a few minutes. The high scattering intensities were particularly obvious for dB1 samples, purified with Ni^{2+}-agarose only (Figure 1a). The purity of these samples was estimated at approximately 95%. Samples with a higher purity, achieved by means of an additional preparative high performance liquid chromatography (HPLC) purification, resulted in lower scattering intensities (see also SANS article). Figure 1b illustrates this observation, but there is still a considerable amount of large aggregates, that contributes roughly 50% to the total scattering signal. The signal coming from large particles or aggregates was further decreased to $\sim$ 20% by using a 10–20 m*M* acetate buffer instead of a phosphate buffer (Figure 1c). The highest monodispersity was obtained in a combined acetate/EDTA buffer at pH 4.2 of two-step purified samples (Figure 1d). Higher concentrations of buffer components did not influence the aggregation behavior of the protein significantly. Further evidence for monodispersity in the acetate/EDTA buffer during a longer time interval was given by the similarity of first, second, and third cumulant analysis at different scattering angles (Figure 2). The observed diffusion coefficient was dependent on the protein concentration, but dB1 samples in acetate/EDTA buffers remained monodisperse at concentrations up to 15 mg/mL. A set of four different types of carboxylate buffers covering the pH range 2–10, yielded diffusion coefficients comparable to those in acetate/EDTA at pH 4, suggesting negligible amounts of aggregates (see Materials and Methods).

Determination of D_0. The observed diffusion coefficients at 20°C, D_{20}, of dB1 and dB4 showed a linear dependence on the concentration, as shown in Figures 3a,b. The concentration of the samples was checked spectrophotometrically after the experiments. The diffusion coefficient at infinite dilution at 20°C, D_0, was estimated through extrapolation to zero concentration, yielding $65.5 \pm 2.8 \times 10^{-12}$ $m^2 \cdot s^{-1}$ for dB1 and $39.4 \pm 0.6 \times 10^{-12}$ $m^2 \cdot s^{-1}$ for dB4. The dissimilar concentration dependences of D_{obs} for dB1 and dB4 can be explained by differences in diffusion behavior of proteins at higher concentrations. Depending on the

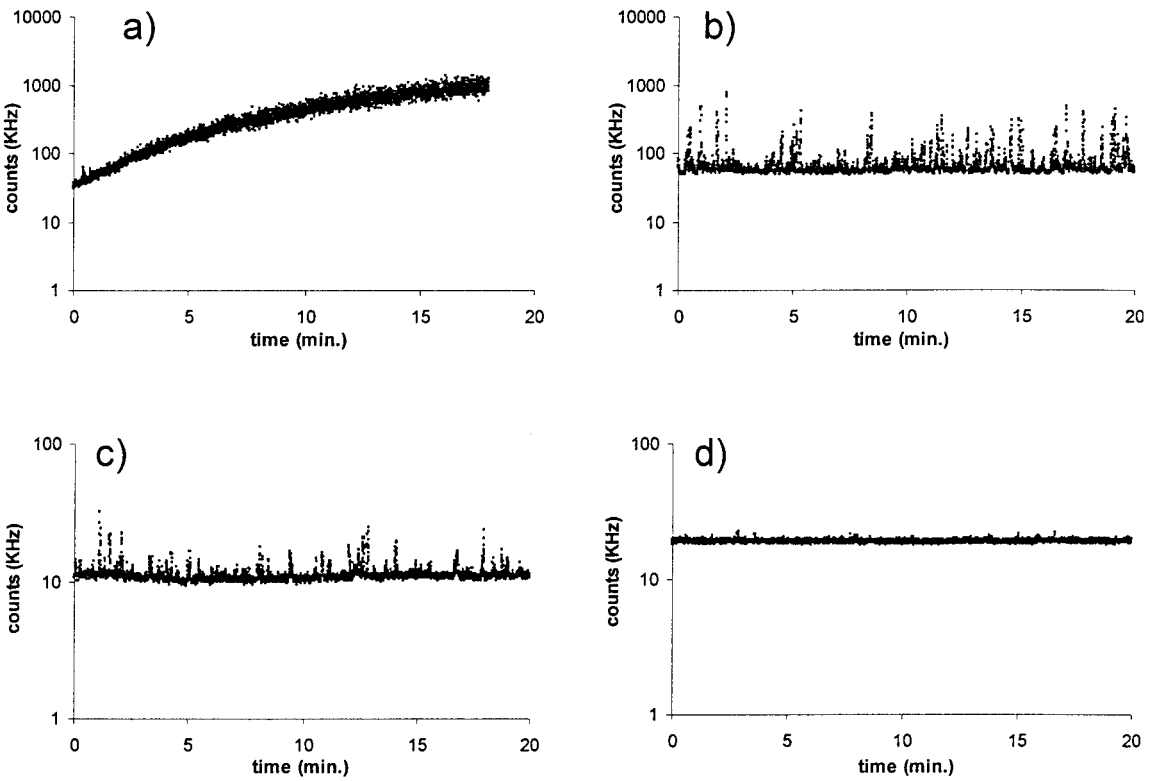

FIGURE 1 Screening of buffers containing dB1 with dynamic light scattering. Photon count rates vs time at 20.0°C of 3–7 mg/mL dB1 solved in four different buffers: (a) 20 m*M* Na-phosphate, pH 4.5, (b) 10 m*M* Na-phosphate, pH 7.0, (c) 10 m*M* Na-acetate, pH 4.25, (d) 10 m*M* Na-acetate, 2 m*M* EDTA, pH 4.2. The purity of the sample under a) was estimated at 95% or higher, the purity of the other samples was >99% pure. See Figure 2 and Materials and Methods for further experimental conditions.

length scale, one can distinguish collective diffusion and self-diffusion, leading to either a positive or negative slope, as observed for dB1 and dB4 respectively.[1]

Analytical Ultracentrifugation

Sedimentation Equilibrium. Sedimentation equilibrium experiments were conducted to determine the molecular masses of dB1 and dB4. Equilibrium data of dB1, collected at three concentrations and three different rotor speeds in acetate/EDTA buffer, are shown in Figure 4 (Beckman XL-1). All nine data sets were subjected to global analysis and fitted best to a model of a single homogeneous sedimenting species, with an apparent molecular mass of 17.35 ± 0.99 kDa, which is slightly higher than the theoretical mass of 16.9 kDa. The residuals in Figures 4a–c indicate that equilibrium was reached. In contrast to the acetate/EDTA solutions, analysis of equilibrium sedimentation data of dB1, recorded in phosphate buffer on the Beckman XL-A, yielded molecular masses

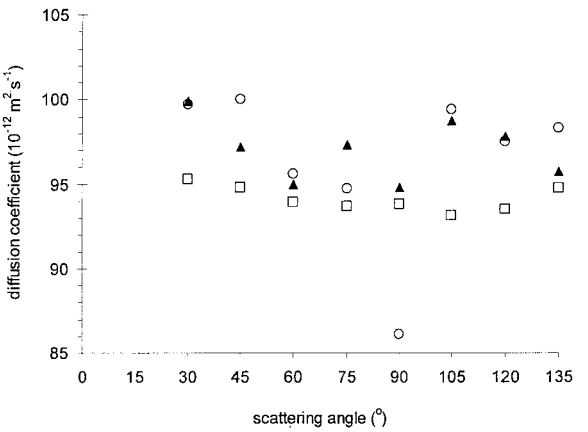

FIGURE 2 Screening in buffers of dB1 with dynamic light scattering. The amount of 4.2 mg/mL dB1 sample in a buffer of 10 m*M* acetate, 2 m*M* EDTA at pH 4.2. Diffusion coefficients from first (□), second (▲) and third (○) order cumulant fits as function of scattering angle. The recorded scattering was the average of three runs of 30 min at each angle.

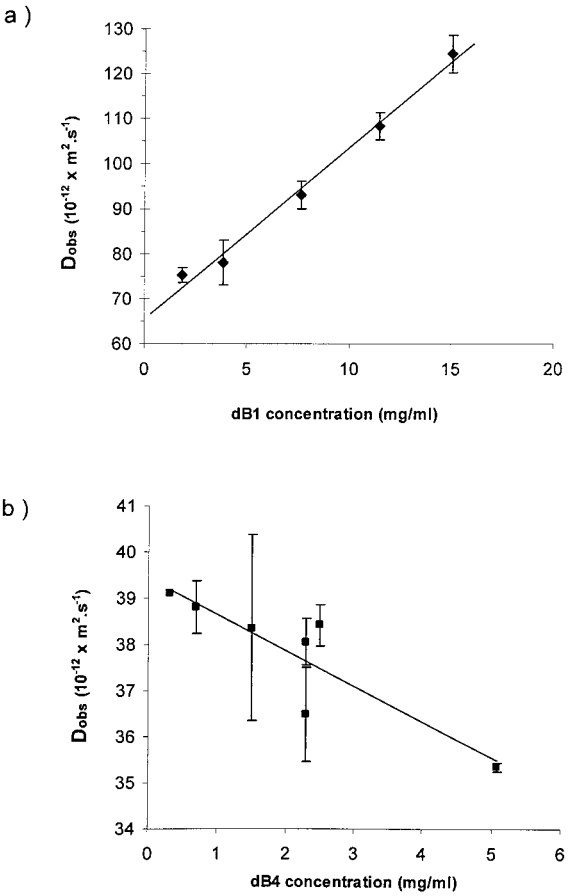

FIGURE 3 Dynamic light scattering, performed at 20°C. (a) D_{obs} of dB1 vs protein concentration in 10 mM acetate, 2 mM EDTA, pH 4.2. (*b*) D_{obs} of dB4 vs protein concentration in 10 m*M* acetate, 2 m*M* EDTA, pH 4.2. Each point in the figure represents the average value of a set of measurements at both 30° and 90° scattering angle. The standard deviation for each point is indicated with error bars.

ranging from 11.7 to 16.0 kDa. The nonlinearity of the r^2 vs ln(A) graphs, together with the lower slope in the low concentration part of the curves, indicate that an equilibrium gradient was not reached in these samples.[2] Equilibrium runs of dB4 in phosphate buffer (Beckman XL-A) also yielded nonlinear r^2 vs ln(A) graphs, indicating unstable solutions as well. The M_w's ranged from 46.3 to 64.1, suggesting similar behavior, as observed for dB1 in phosphate buffers (M_{dB4} = 63.8 kDa). All samples remained visually transparent during the equilibrium runs.

Sedimentation Velocity. Sedimentation coefficients for dB1 were determined at 20°C in two different buffers. The observed s_{20} values for the two dB1 samples in acetate/EDTA buffer were 1.43 S (dB1 conc. 0.49 mg/mL) and 1.49 S (dB1 conc. 1.48 mg/mL). The 1.21 mg/mL dB1 sample in phosphate buffer yielded 1.45 S. The extrapolated value at infintite dilution, s_0, was determined to be 1.40 ± 0.02 S for dB1. Velocity runs performed on three dB4 samples in phosphate buffer, with dB4 concentrations 0.07, 0.16, and 0.32 mg/mL, resulted in s_{20} values of 2.93, 3.05, and 3.09 S. The extrapolated value at infintite dilution, s_0, was determined to be 2.91 ± 0.04 S for dB4. In addition, a sedimentation velocity experiment of dB1 in phosphate at a lower speed was performed, in which the diffusion of the boundary was followed in time. The diffusion coefficient from the resultant fit was 69.5 ± 5.2 × 10^{-12} $m^2 \cdot s^{-1}$.

DISCUSSION

Monodispersity

The DLS results have demonstrated that the highest levels of monodispersity were obtained for dB1 and dB4 in acetate/EDTA solutions. The sedimentation

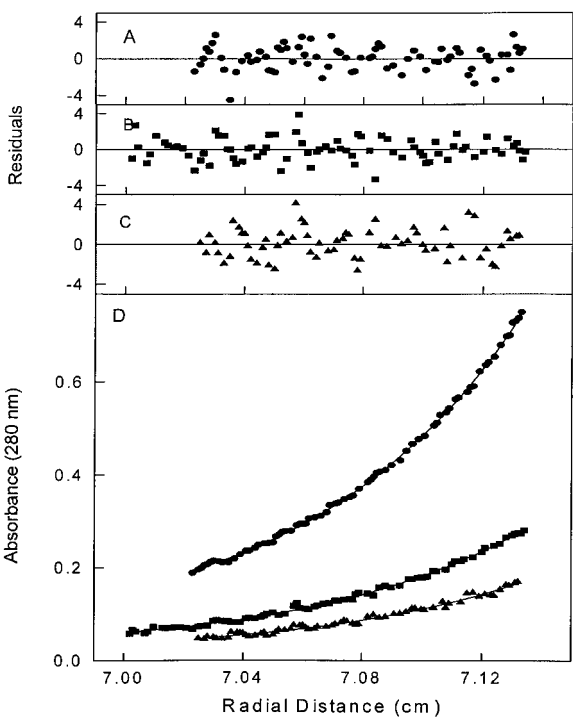

FIGURE 4 Sedimentation equilibrium profiles of dB1. (D) The equilibrium profiles for dB1 at 28000 rpm with three initial concentrations, 0.081 (▲), 0.163 (■), and 0.49 (●) mg/mL. The solid lines represent the best fits described by the global analysis of all nine data sets. The residuals of the fits are shown in A–C for the data sets with initial concentrations of 0.49, 0.163, and 0.081, mg/mL, respectively.

equilibrium experiments evidenced that under these conditions no aggregates or oligomers could be detected in dB1 and dB4 solutions. The presence of aggregates was detected in phosphate solutions, as demonstrated by the substanstially higher scattering and instabile sedimentation equilibrium. Previous reports suggested that the abundant glutamine side chains form intermolecular hydrogen bonds.[3] Obviously, a high purity and the presence of acetate and EDTA decreases the intermolecular interactions of dB1 monomers, as evident from the differences in scattering intensities (Figures 1a–d). The carboxylate groups possibly interact with the glutamines, preventing intermolecular hydrogen bonding. The fact that the chemical structure of the buffer is important, but not the pH, is compatible with this conclusion.

The dominating contribution in the scattering signal from the polymeric particles in phosphate solutions could give a wrong picture of the numerical fraction of these particles. To estimate the relation between the hydrodynamic radius and the scattering intensity of a particle, the scattering intensities of dB1 and dB4 solutions were compared. A dB4 molecule scatters a factor 15.6 more intensity than a dB1 molecule, as determined from concentrations plots at identical scattering angle (30°). The scattering intensity is proportional to $M_w^{2.07}$, which nicely corresponds to the quadratic relation predicted by theory.[4] Assuming that aggregates are spherical and that their partial specific volumes are comparable with the dB1 and dB4 monomers, the scattering intensity is proportional to $R^{6.2}$ (radius of the particle). Using this relation, the highly scattering sample in Figure 1a would only contain 3 aggregates of 170 nm size, against 1 billion of monomeric particles. Although a rough calculation, it illustrates that even in phosphate buffers, the amount of aggregates is still negligible compared to the amount of monomers. Nevertheless, such amounts disturb scattering experiments, so that the use of acetate/EDTA buffers was required. For sedimentation velocity runs, the interpretation of physical values is not hampered by the large aggregates present in phosphate, due to the linear relation between absorption and molecular mass, and the physical separation of these populations in the cuvette. This is compatible with the observed monomeric molecular masses in both phosphate and acetate/EDTA buffers calculated from the r^2 vs ln(A) plots of the sedimentation equilibrium data.

Calculation of Molecular Masses and Frictional Ratios

The combined scattering and sedimentation results demonstrate that s_0 and D_0 describe the hydrodynamic behavior of dB1 and dB4 monomers in solutions. Direct evidence of agreement between the two types of hydrodynamic techniques is shown by the similarity of D_0 values determined for dB1 in the DLS and sedimentation boundary experiments. Additional proof is delivered by the molecular masses determined from the two sets of s_0 and D_0 values, using the Svedberg equation:

$$\frac{s_0}{D_0} = \frac{M(1 - \nu\rho)}{RT} \tag{1}$$

in which M is the molecular mass, ν the partial specific volume of the protein, ρ the density of the solvent, R the gas constant, and T the temperature. The outcome is 16.7–19.1 kDa for dB1 and 60.0–63.8 for dB4, using the tolerances of the extrapolated s_0 and D_0 values. Both ranges fit very well with the calculated molecular masses of 16.9 and 63.8 kDa.

Figure 5 shows the experimental s_0 values of dB1 and dB4, corrected for partial specific volume, ν, as function of molecular mass. Values of 37 reference proteins with various shapes and sizes are included in this graph. Globular proteins can be expected on or near the diagonal, whereas nonglobular proteins are off-diagonal.[2] Normally, the distance from the diagonal in this type of plot increases with the asymmetry and/or friction of the protein. Also, s_0 values of dB1 and dB4 are relatively low, which indicates slow transport properties (Figure 5). Similar conclusions were drawn from their diffusion coefficients, in comparison with those of a set of reference proteins (data not shown), and from the high SDS molecular masses (see SANS article). More sophisticated analysis of size and shape can be made by examination of the frictional ratio, f/f_0. This parameter represents the extra friction of a particle encountered, compared to an unhydrated sphere of equal volume. The reference proteins with the 10 highest f/f_0 values, ranging from 1.42 to 2.00, have the most distant position from the diagonal. The f/f_0 values of dB1 and dB4 were calculated from s_0 values, using Svedberg and Stokes relations,

$$\frac{f}{f_0} = \frac{1}{s_0} \times \frac{M(1 - \nu\rho)}{6\pi\eta N_A} \times \left(\frac{4\pi N_A}{3M\nu}\right)^{1/3} \tag{2}$$

and from D_0 values, using the Stokes–Einstein relation,

$$\frac{f}{f_0} = \frac{1}{D_0} \times \frac{k_B T}{6\pi\eta} \times \left(\frac{4\pi N_A}{3M\nu}\right)^{1/3} \tag{3}$$

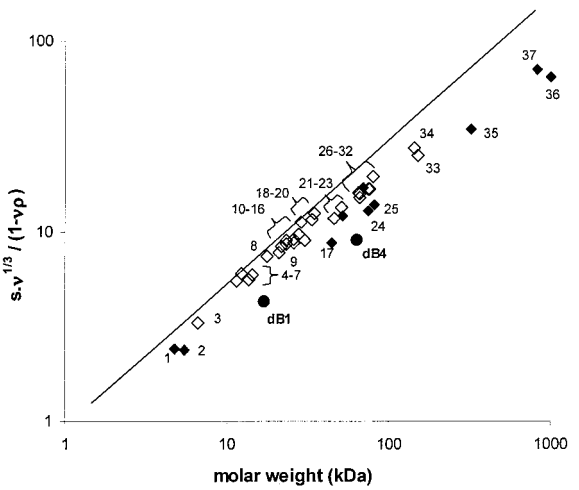

FIGURE 5 Hydrodynamic analysis. Double logarithmic plot with s_0 values of dB1, dB4, and reference proteins, corrected for partial specific volume, ν, as function of molecular mass. A set of 37 values of reference proteins with various shapes and sizes was extracted from Fasman[23] and Squire and Himmel.[24] The dB1 and dB4 are indicated explicitly in the figure, the reference proteins with (◆) for the ten highest f/f_0 values, or (◇) for the remaining proteins. The numbers indicate the following: (1) human γ2 globulin; (2) bovine ACTH; (3) bovine pancreatic trypsin inhibitor; (4) human β2-microglobulin; (5) bovine ribonuclease A; (6) hen lysozyme; (7) equine cytochrome C; (8) sperm whale myoglobin; (9) human retinol-binding protein; (10) procine adenylate kinase; (11) bovine trypsin; (12) bovine trypsinogen A; (13) human Bence–Jones protein RE1; (14) human B1-glycoprotein; (15) procine elastase; (16) B. amyloliq. Subtilisin; (17) human orosomucoid; (18) human carbonic anhydrase B; (19) bovine superoxide dismutase; (20) bovine carboxypeptidase A; (21) yeast phosphoglycerate kinase; (22) human transcortin binding globulin; (23) jack bean concanavalin A; (24) human plasmin; (25) human plasminogen; (26) human albumin; (27) bovin serum albumin; (28) equine hemoglobin-oxy; (29) porcine malate dehydrogenase; (30) human transferrin; (31) human factor II coag.; (32) equine alcohol dehudrogenase; (33) human Immunoglobulin (Ig) G; (34) dogfish lactate dehydrogenase; (35) human plasma factor XIII; (36) human plasma (Ig) M; (37) human α-macroglobulin.

in which η is the viscosity, N_A Avogadro's number, and k_B the Boltzmann constant.

The calculated f/f_0 values from s_0 and D_0 nicely overlapped (Table I). The results are in line with earlier viscosimetric work on the HMW protein Bx7, where it was suggested that the protein exists either as highly solvated random-coiled chains or as relatively asymmetric particles.[5] The hydration was introduced in the hydrodynamic analysis, by decomposition of f/f_0 into the form factor, f/f_{sp}, and the hydration factor, f_{sp}/f_0, according to

Table I Frictional Ratios f/f_0 Determined from s_0 and D_0

	S_0	D_0	Consensus
dB1	1.81–1.86	1.83–2.03	1.83–1.86
dB4	2.09–2.15	2.02–2.09	2.09

$$\frac{f}{f_0} = \frac{f}{f_{SP}} \times \frac{f_{SP}}{f_0} = \frac{f}{f_{SP}} \times \left[\frac{\nu + \delta/\rho}{\nu}\right]^{1/3} \quad (4)$$

in which f_{sp} represents the frictional coefficient of a hydrated sphere of equal volume and δ the mass fraction of hydrated water, relative to the protein. Even with an extremely high δ of 2.00 $g_{H_2O}/g_{protein}$, both proteins cannot be described by a sphere that has a form factor of 1, as shown by the form factor vs hydration δ in Figure 6.

Shape Modeling

The WLC model was purported to be the correct model for dB1 and dB4 in the SANS article. The high flexibility of both molecules was demonstrated by the low persistence length l_p (SANS data), as well as the gradual urea denaturation of dB1, demonstrated by van Dijk et al.[3] The WLC model was tested using the hydrodynamic results, as well as the contour lengths of 235 Å (dB1) and 900 Å (dB4), and the persistence length of 13 Å (dB1 and dB4), obtained with SANS and small angle x-ray scattering (SAXS). The frictional coefficient, f, was calculated for both dB1 and dB4 from the WLC dimensions, using a set of well-known numerical equations, for the unperturbed worm-like chain.[6] Given the f values, s_0 and D_0 were

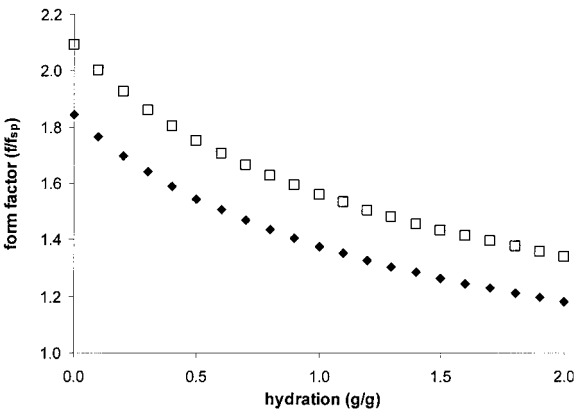

FIGURE 6 Form factors of dB1 (◆) and dB4 (□) vs hydration.

calculated from Svedberg and the Stokes–Einstein equations, respectively.

A combined grid search on s_0 and D_0 of dB1 and dB4 yielded a diameter, *d,* of 27 ± 4 Å and a persistence length, l_p of 19 ± 2 Å. Both values are slightly higher than SANS-derived dimensions of 15 and 13 Å, respectively. An apparent higher l_p is expected, since Yamakawa's model does not account for excluded volume effects. Furthermore, the SANS diameter represents the unhydrated dB1 and dB4, due to the low contrast difference between bulk and bound water molecules. Hydrodynamic parameters represent the hydrated proteins, which could explain the larger diameter. If the volume of a bound water molecule is estimated at 24.5 Å^3, the diameter equals 3.6 Å.[7] The increase of the diameter of the WLC due to one hydration layer is then 7.2 Å. In our model, this would correspond to 1–2 water layers. An exact treatment of these effects on the transport properties of particles can be pursued by renormalization group methods, but will not be further pursued in this paper.[8,9]

The dB1 and dB4 molecules possess identical secondary structures (CD) and amino acid compositions. In fact, dB1 and dB4 can be seen as two representatives of a homologuous series of polymer fractions. The dependence of hydrodynamic parameters on the molecular mass of polymers has been described by the so-called Mark–Houwink–Kuhn–Sakurada (MHKS) coefficients,[10]

$$s_0 = K' \times M^b \tag{5a}$$

$$D_0 = K'' \times M^\varepsilon \tag{5b}$$

$$R_G = K''' \times M^c \tag{5c}$$

in which the coefficients and proportionality factors, $K,'$ $K,''$ and K''' are constant for a given polymer + solvent system.[8] The coefficients *b,* ε, and *c* were calculated to be 0.55, 0.39, and 0.66 from the experimental s_0, D_0, and R_G values, respectively. These values are most compatible with a random coil structure.

Based on the scattering and hydrodynamic results, the stiff ellipsoid of revolution model for dB1 and dB4 is unlikely. Since dB1 and dB4 have an identical local structure, a long axis ratio of dB4/dB1 ~ 4 is expected, if the shape would correspond to an extended structure. The calculated ratios of 1.4 for the prolate and 1.5 for the oblate ellipsoids are, however, much lower. Following the same line of thought, a value of 1.4–1.5 is found for the rod-like shape (hydration range 0.0–1.0 $g_{H_2O}/g_{protein}$). These outcomes clearly do not favor the prolate, oblate or rodlike models. For further backgrounds on shape modeling and calculations, see Refs. 1, 10, and 11.

CONCLUSION

Our results question the earlier models of the "stiff" extended shapes.[4,12,13] For the first time, hydrodynamic parameters have been obtained on monodisperse samples of the repetitive HMW domain that enabled the interpretation of the monomeric size and shape. Aggregation was controlled using carboxylate buffers. Presumably, the caboxylate moieties form strong H-bonds with the glutamines, and thereby suppress intermolecular H-bonding, which leads to aggregates. The successful matching of two separately obtained hydrodynamic parameters of dB1 and dB4 in the WLC model treatment provides further evidence for this model. The small discrepancy between the hydrodynamic and scattering data, possibly coming from an excluded volume effect, could be compensated by a solvation layer of 1–2 water molecules thick around the protein. It is compatible with the high solubility of dB1 up to ~ 60 mg/mL,[14] and with the high hydrophilicity of −1.9 for dB1 and dB4, calculated from amino acid composition.[15] The solvation of the central domain is much higher than those of the terminal domains of the HMW subunits.[16,17] This difference emphasizes the dual role of HMW wheat gluten proteins in water binding and aggregation.

MATERIALS AND METHODS

Dynamic Light Scattering

DLS was applied in order to define conditions that resulted in monodisperse protein samples for SANS experiments. We used an instrument consisting of a light-scattering goniometer equipped with a 500 mW argon-ion laser.[18] The scattered light intensity was detected by a photomultiplier. An intensity autocorrelation was obtained from the photon pulses. Diffusion coefficients were obtained from the resulting autocorrelation curves with cumulant fitting, using ALV-5000/E software, version 2.6.1. Hydrodynamic radii of spheres of the same volume were calculated from the Stokes–Einstein relation. The NaAc buffer concentration ranged from 10 to 50 m*M* and all samples contained 3 m*M* EDTA. Three other buffers, all containing carboxylate groups, but with pHs deviating from the acetate/EDTA buffer, were tested; trifluoroacetate, pH 2.0; maleate/Tris, pH 6.5; and carbonate/NaOH, pH 9.6. The concentration series of dB1 and dB4 experiments were performed at static scattering angles of 30° and 90° at 20.0°C. The dB1 dissolved in 50% aqueous propanol or high-salt (0.5*M* NaCl) induced visually observable aggregation, and was not fur-

ther examined. All samples were filtered on 0.1 μm Millipore filters prior to measurement in order to remove dust.

Analytical Ultracentrifugation

Sedimentation equilibrium and sedimentation velocity experiments were performed in a Beckman XL-A or XL-I analytical ultracentrifuge, equipped with ultraviolet absorption optics. All experiments were carried out at a temperature of 20.0°C. The wavelength was chosen between 220 and 280 nm in order to obtain an absorption (0.2–0.8 optical density), which was linear with the protein concentration. The samples were dissolved either in 10 m*M* Na-phosphate buffer, pH 6.0, containing 150 m*M* NaCl or in 10 m*M* acetate, 2 m*M* EDTA, pH 4.2, containing 100 m*M* NaCl, as indicated in the figures. Salt was added to compensate for the electrolyte effect. The protein concentrations were determined by absorbance at 280 nm, using a molar extinction coefficient of 1.444 $\times$ E4 L $\cdot$ mol^{-1} $\cdot$ cm^{-1}, as calculated from the amino acid composition.[19] The partial specific volumes, v_{sp}, of dB1 and dB4, were calculated from the amino acid composition as 0.697 and 0.699 mL/g, respectively.[7,20] Sedimentation equilibrium experiments on dB1 in acetate/EDTA buffers were performed at concentrations of 0.081, 0.163, and 0.49 mg/mL at rotor speeds of 20,000, 24,000, and 28,000 rpm with the Beckman XL-I. Sedimentation data were acquired every 0.001 cm with ten replicates and then averaged after reaching equilibrium. To obtain the apparent molecular mass the data sets at multiple speeds and concentrations were simultaneously analysed using the Beckman data analysis software. Sedimentation equilibrium runs of dB1 and dB4 samples in phosphate buffers were run at 28,000 and 15,000 rpm respectively, on the Beckman XL-A using the conventional method of Chervenka.[21] The sample volume in the cuvettes was 100–120 μL Absorption spectra were recorded after 15 h (no residuals calculated).

Sedimentation velocity experiments were carried out at 48,000 rpm on two dB1 samples in acetate/EDTA buffer (1.48 and 0.49 mg/mL) on the Beckman XL-1. Data were collected in the continuous mode with a radial stepsize of 0.003 cm, at 10-min intervals on 400 μL samples loaded into double sector centerpieces. Data on a third dB1 sample (1.21 mg/mL) were recorded in phosphate buffer at 56,000 rpm in a run of approximately 3 h, at 25–min intervals. Three dB4 samples, with concentrations 0.09, 0.19, and 0.37 mg/mL in phosphate buffer, were recorded on the Beckman XL-A at 56,000 rpm, at $\sim$ 25-min intervals. All observed sedimentation coefficients were determined using the Beckman data analysis software. For theory and further backgrounds see the classical sources (Refs. 11 and 22) or more recent references (Refs. 2 and 10). The diffusion coefficient $D_{20,w}$ of a 3.4 mg/mL dB1 sample at 22.0°C, was determined on a Beckman model-E ultracentrifuge, equipped with a Schlieren detection system.

The authors wish to thank Ariel Koch from the University of Basel for the performance of sedimentation experiments and Jan Klok of the NIZO Ede for his assistance during the *DLS* experiments. Stimulating discussions with Stefan Egelhaaf were useful for integration of the SANS data (first paper) with the hydrodynamic experiments. The Dutch Ministry of Economic Affairs supported this research, project IOP-IE92014.

REFERENCES

1. de Kruif, C. G. Langmuir 1992, 8, 2932–2937.
2. van Holde, K. E.; Johnson, W. C.; Ho, P. S. Principles of Physical Biochemistry; Prentice Hall: Englewood Cliffs, NJ, 1998.
3. van Dijk, A. A.; de Boef, E.; Bekkers, A. C. A. P. A.; van Wijk, L. L.; van Swieten, E.; Hamer, R. J.; Robillard, G. T. Protein Sci 1997, 6, 649–656.
4. Pecora, R. Dynamic Light Scattering, Applications of Photon Correlation Spectroscopy; Plenum Press: New York, 1985.
5. Field, J. M.; Tatham, A. S.; Shewry, P. R. Biochem J 1987, 247, 215–221.
6. Yamakawa, H.; Fujii, M. Macromolecules 1973, 6, 407–415.
7. Perkins, S. J. Eur J Biochem 1986, 157, 169–180.
8. Fujita, H. Macromolecules 1988, 21, 179–185.
9. Oono, Y.; Kohmoto, M. J. J Chem Phys 1983, 78, 520–528.
10. Harding, S. E. Biophys Chem 1995, 55, 69–93.
11. Tanford, C. Physical Chemistry of Macromolecules; John Wiley & Sons; New York, 1961.
12. Matsushima, N.; Danno, G.; Sasaki, N.; Izumi, Y. Biochem Biophys Res Commun 1992, 186, 1057–1064.
13. Thomson, N. H.; Miles, M. J.; Popineau, Y.; Harries, J.; Shewry, P. R.; Tatham, A. S. Biochem Biophys Acta 1999, 1430, 359–366.
14. van Swieten, E. Ph.D. thesis. Groningen University, The Netherlands, 2001.
15. Kyte, J.; Doolittle, R. F. J Mol Biol 1982, 157, 105–132.
16. van Dijk, A. A.; van Swieten, E.; Kruize, I. T.; Robillard, G. T. J Cereal Sci 1998, 28, 115–126.
17. Bekkers, A. C. A. P. A.; de Boef, E.; van Dijk, A. A.; Hamer, R. J. J Cereal Sci 1999, 29, 109–112.
18. Rouw, P.; de Kruif, C. G. J Chem Phys 1988, 88, 7799–7806.
19. Pace, C. N.; Vajdos, F.; Fee, L.; Grimsley, G.; Gray, T. Protein Sci 1995, 4, 2411–2423.
20. Harpaz, Y.; Gerstein, M.; Clothia, C. Structure 1994, 2, 641–649.
21. Chervenka, C. H. A Manual of Methods for the Analytical Ultracentrifuge; Beckman Instruments; Palo Alto, CA 1970.
22. Svedberg, T.; Pedersen, K. O. The Ultracentrifuge; Oxford University Press: London, 1940.
23. Fasman, G. Handbook of Biochemistry and Molecular Biology, 3rd ed.; CRC Press; Cleveland, OH, 1976.
24. Squire, P. G.; Himmel, M. E. Arch Biochem Biophys 1979, 196, 165–177.